DOI：10.13234/j.issn.2095-2805.2025.7.1 **中图分类号**：TM46 **文献标志码**：A

反激变换器电磁干扰研究综述

姚俊涛，王 硕
(美国佛罗里达大学电力电子与电能研究实验室，盖恩斯维尔 佛罗里达州 32611)

(特邀论文)

摘要：在消费类和商用产品中，反激式变换器必须遵守相关传导和辐射电磁干扰EMI(electromagnetic interference)的严格标准。随着高速宽禁带WBG(high-speed wide bandgap)半导体器件在现代电力电子中的普遍应用，系统布局越来越紧凑，EMI的管理变得日益复杂。本文综述了针对传导EMI的成熟建模技术与抑制策略，重点分析了差模DM(differential mode)和共模CM(common mode)噪声，以及反激式变换器中的辐射EMI。讨论内容涵盖了器件级设计和变换器系统优化2个层面的解决方案。

关键词：反激式变换器；电磁干扰；传导电磁干扰；辐射电磁干扰；差模；共模

An Overview of EMI Research in Flyback Converters

YAO Juntao, WANG Shuo
(Power Electronics and Electrical Power Research Lab, University of Florida, Gainesville, FL 32611, USA)

(*Invited Paper*)

Abstract: Flyback converters in consumer and commercial products must adhere to strict regulatory standards for conducted and radiated electromagnetic interference (EMI). Managing EMI has become increasingly complex in modern power electronics, particularly with the integration of high-speed wide bandgap (WBG) devices into compact system layouts. A review of established modeling techniques and mitigation strategies for conducted EMI is presented, focusing on differential mode (DM) and common mode (CM) noise, alongside radiated EMI in flyback converters. The discussion encompasses solutions at both component-level design and converter system optimization.

Keywords: Flyback; EMI; conducted EMI; radiated EMI; differential mode (DM); common mode (CM)

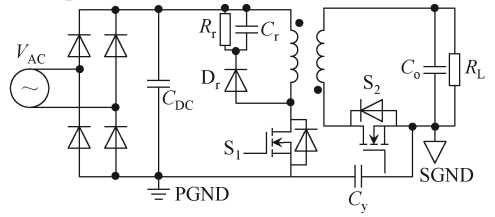
1 Introduction

Flyback converters are very popular in both consumer and commercial products such as power adapters and auxiliary power supplies. Due to their switching mode operations, flyback converters generate both conducted and radiated electromagnetic interference (EMI). In many applications, EMI standards such as CISPR25, CISPR32, DO-160, MIL-461, etc., are enforced on flyback converters[1] for both conducted and radiated EMI. To meet these EMI standards, EMI filters are usually employed to mitigate EMI at the price of increased size and increased cost.

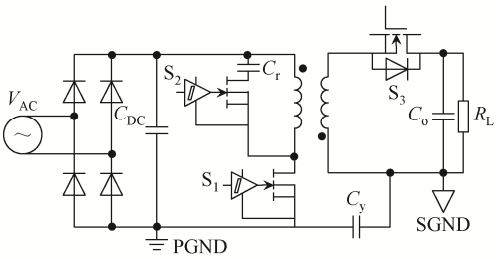
A conventional flyback topology is shown in Fig. 1(a). Soft switching techniques have been implemented in resonant-mode flyback converters[2], active clamp flyback (ACF) converters[3-5], and asymmetrical half-bridge flyback converters[6-7]. ACF converters have been commercialized to improve efficiency by recycling the energy in the leakage inductance, to minimize the transient ringing, and to reduce the voltage stress[3-4] of the switching devices, as in Fig. 1(b).

收稿日期：2025-07-22；**录用日期**：2025-09-22；**网络首发日期**：2025-11-18

Recently, WBG devices have become popular in flyback converters to achieve high-power-efficiency and high-power-density[3-4]. However, the high switching speeds and high switching frequencies of WBG devices increase HF switching EMI noise and near-field EMI couplings, resulting in significant EMI challenges[8]. To address these challenges, it is critical to understand and reduce the EMI by developing EMI models and reduction techniques for both conducted and radiated EMI.



(a) Conventional flyback converter



(b) ACF converter

Fig. 1 Topologies of flyback converters

Traditionally, the conducted EMI is categorized into differential mode (DM) and common mode (CM) EMI. The DM EMI flows between power delivery paths and CM EMI flows between power delivery paths and the ground or metal chassis.

Conducted EMI modeling research focuses on EMI noise sources, EMI propagation paths, and component models[1,9-10]. EMI noise source modeling focuses on identifying and characterizing EMI noise sources. EMI propagation modeling focuses on identifying major EMI propagation paths, and developing models for mutual inductive or capacitive couplings[11-14] between noisy loops or nodes and noise-sensitive loops or nodes, and extracting parasitic parameters, etc. Component modeling focuses on developing high-frequency (HF) parasitic models for components on EMI propagation paths and characterizing their EMI performance[1,15-16].

Conducted EMI reduction research focuses on EMI filter design and optimization, improving component EMI performance with parasitic cancellation, mutual coupling reduction, CM EMI balancing, etc., which are developed based on the EMI modeling research above.

Radiated EMI modeling research[17-19] focuses on developing radiated EMI models to understand the radiation mechanism in flyback converters[17], radiated EMI noise source modeling, developing component parasitic models and characterizing their performance for radiated EMI, exploring mutual couplings and their impacts on radiated EMI, etc.

Radiated EMI reduction research[17-20] focuses on radiated EMI filter design, mutual coupling reduction techniques, shielding techniques, PCB layout optimization, and component design optimization, etc.

This paper summarizes and examines recent advancements in EMI modeling and mitigation techniques for flyback converters, as illustrated in Fig. 2. Section 2 focuses on conducted EMI, Section 3 addresses radiated EMI, and Section 4 discusses future research and concludes the survey.

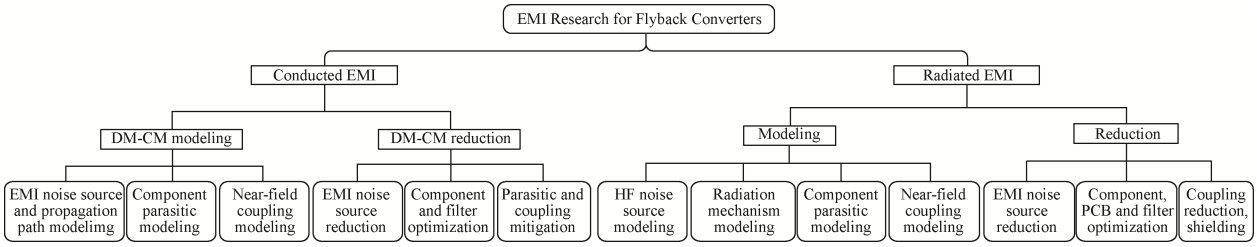


Fig. 2 Modeling and reduction of conducted and radiated EMI in flyback converters

The major efforts of this paper include: (1) a comprehensive review of modeling and mitigation tech-

niques for conducted EMI in flyback converters from component to system levels; (2) an overview of recent advancements in analyzing and reducing radiated EMI in flyback converters.

2 Modeling and Reduction of Conducted EMI

The EMI propagation paths of conducted DM and CM EMI in an AC-DC flyback converter are illustrated in Fig. 3. DM noise is emitted from the main switch S_1 and then attenuated by DC bus capacitor C_i. It further flows through the diode bridge and is attenuated by the DM EMI filter before circulating back through the line impedance stabilization networks LISNs[9]. CM noise, on the other hand, has two propagation paths. For the 1st path, it is emitted from the drain of MOSFET (main switch) S_1 and then flows through the interwinding parasitic capacitance between transformer windings to the secondary ground (SGND). It further flows through the parasitic capacitance C_{SG} between the secondary SGND and the ground to the earth ground. While for the 2nd path, the CM EMI originates from the drain of MOSFET to the heat sink via the parasitic capacitance between the drain of the MOSFET and the heatsink and subsequently to earth ground via the parasitic capacitance between the heatsink and the earth ground. The second path can be eliminated by grounding the MOSFET's heatsink to the primary ground (PGND), making the first path a dominant contributor to CM noise. Therefore, it is essential to model and mitigate this primary CM noise.

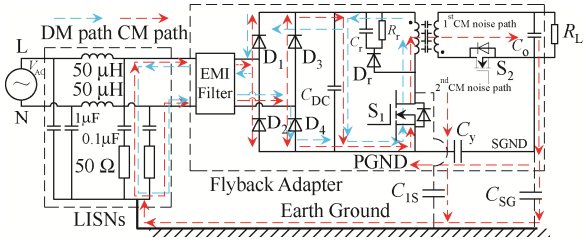


Fig. 3 DM-CM noise propagation paths in an AC-DC flyback converter

2.1 Modeling and Reduction of Conducted DM EMI

2.1.1 DM EMI Modeling

The existing DM EMI modeling primarily focuses on developing DM models for flyback converters, analyzing DM EMI due to the reverse recovery currents of the diode bridge, developing parasitic models for DM EMI filters and components, and characterizing the impacts of parasitic couplings. The EMI models for the conventional and ACF flyback converters with either an AC EMI filter or a DC-bus EMI filter[11-12] in Fig. 1(a) and (b) are developed in Fig. 4(a) and (b) by substituting switching devices with voltage sources or current sources based on network theory. Although various substitutions are possible, only those convenient for DM noise analyses are preferred.

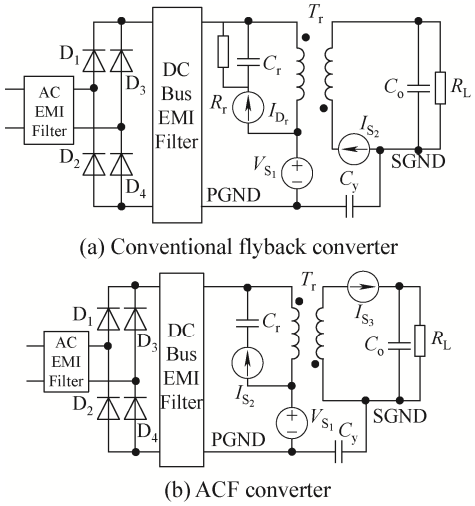


Fig. 4 DM models of flyback converters[11-12]

It was found that a DC-bus filter (π-type) has the benefits of smaller DM inductors and lower power loss than an AC EMI filter because of the lower peak and root mean square (RMS) currents flowing through the DM inductor than those in the DM inductor of an AC EMI filter[11]. The parasitic model for a DM EMI filter was developed in [21-22]. It was disclosed that the mutual inductance between the inductor and capacitors or between the two capacitors of a π-type filter determined the EMI filter's HF per-

formance. The mutual inductance generally leads to worse HF filtering performance. Two EMI filters with identical topologies and components can exhibit very different HF filtering performance with different mutual parasitic couplings[21-26].

Fig. 5(a) and (b) show the reverse recovery currents of the 50/60 Hz diode rectifier in Fig. 3 during the turn-off of diodes D_1 and D_4 and their impact on the noise voltage drop $V_R = i_R R_{LISN}$ on LISNs. It was disclosed that even though the reverse recovery currents repeat at 50/60 Hz, it can lead to significant DM EMI noise above 150 kHz due to its impact on LISNs and the operating principle of EMC spectrum analyzers[15].

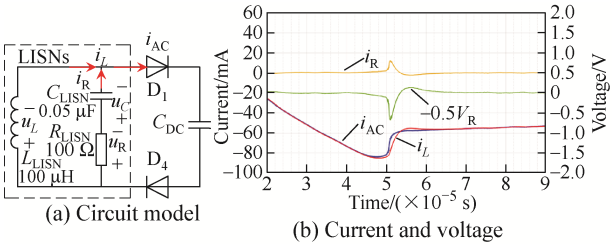


Fig. 5 The voltage spikes on LISNs due to the reverse recovery currents of 50/60 Hz diodes lead to high DM EMI above 150 kHz [15]

The HF impedance model of an EMI filter inductor was explored in [27] and the microscopic electromagnetic phenomena were examined. It was discovered that the electric field inside the magnetic core, which had been long ignored, plays an important role in the inductor's HF EMI filtering performance.

2.1.2 DM EMI Reduction

DM EMI can be reduced either from noise sources or from EMI propagation paths. The techniques are summarized in Table 1.

On the noise source side, the switching noise can be reduced by spreading spectrum with modulations, employing soft-switching or using snubbers to suppress switching ringing[28-39]. The EMI due to the reverse recovery currents of the diode bridge can be reduced by using an X-capacitor or fast-recovery diodes with soft turn-off characteristics. On the EMI propagation paths, EMI filter topologies are designed based on impedance mismatch[41-42] to fully utilize the EMI source and load impedances as part of the EMI filter. At the component level, the inductor core or the number of winding turns can be designed to reduce core loss (so as to increase Z_{EPR}) and reduce electric energy (so as to increase Z_{EPC}) inside the core to achieve high impedance at desired frequencies for EMI reduction, as in Fig. 6[27]. The cancellation technique for inductor winding's equivalent parallel capacitance (EPC) was developed in [23,26,43-45] to reduce HF EMI. Capacitor equivalent series inductance (ESL) and equivalent series resistance (ESR) cancellation techniques were developed in [46] to reduce HF EMI as in Fig. 7. Mutual parasitic coupling cancellation techniques were developed in [26,43,50] to improve EMI filter's HF performance[21], which can greatly reduce the HF EMI as shown in Fig. 8(a) and (b).

Tab. 1 Conducted DM EMI noise reduction techniques

Techniques	Brief description
Noise source reduction	Reducing EMI due to the reverse recovery currents of 50/60 Hz diode rectifier by using fast-recovery diodes with soft turn-off characteristics, or an X-capacitor[15]
	Switching ringing suppression using lossy snubbers[28-29], lossless resonant snubbers[30-33], active snubbers[34-35], and soft-switching techniques[4,36-39], spectrum spreading techniques[40]
EMI filter topology design	Principles of impedance mismatch and insertion loss, EMI filter topologies of LC, π, T, multi-stage, etc.[41-42]
Filter component design	Inductor core and winding design[27], inductor EPC cancellation[23,26,43-45], and capacitor ESL cancellation[46]
Parasitic coupling mitigation	Mitigation of parasitic couplings[21-24,26], inductors with low magnetic emission and EMI immunity[47-49]

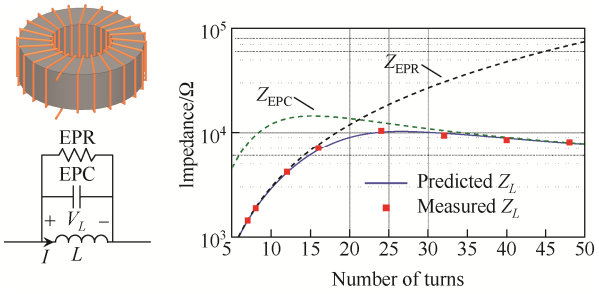
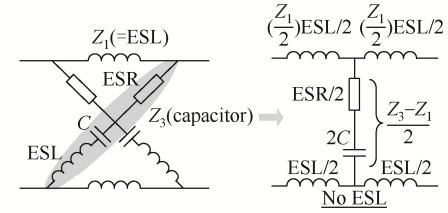
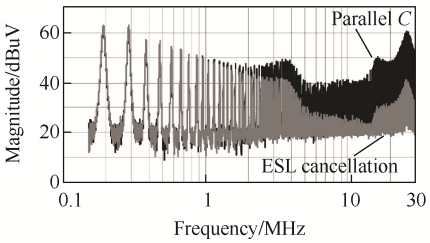


Fig. 6 Inductor winding design for high impedance at desired frequencies[27]

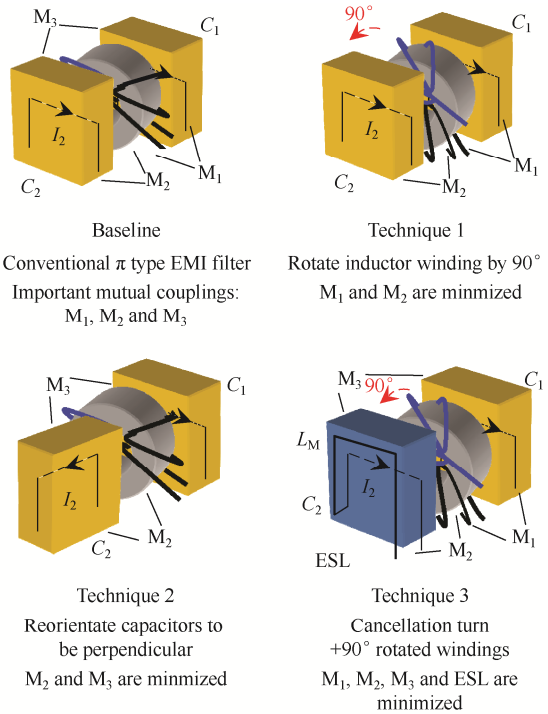


(a) Principle of ESL cancellation

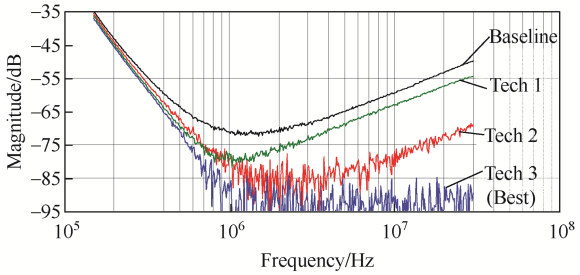


(b) ESL cancellation can greatly reduce HF DM EMI

Fig. 7 ESL cancellation to reduce HF EMI[46]



(a) EMI fulter configurations to reduce parasitic mutual couplings



(b) Comparison of measured insertion gains

Fig. 8 Techniques to reduce parasitic mutual inductance in an EMI filter to improve its HF performance[26,43,50]

2.2 Modeling and Reduction of Conducted CM EMI

2.2.1 CM EMI Modeling

The modeling research for conducted CM EMI primarily focuses on developing CM EMI models for transformers, establishing grounding models for CM EMI filters, and creating parasitic coupling models to account for mutual couplings that contribute to CM EMI noise. The CM EMI models for the flyback converters can be developed based on Fig. 4(a) and (b) by adding CM parasitic capacitance between the voltage pulsating nodes and the earth ground and replacing the transformer with its CM EMI model[1,16,51-52]. Since the CM EMI resulted from the parasitic capacitance between the transformer primary and secondary windings could be much higher than that resulted from the CM parasitic capacitance between the drain of MOSFET (S_1) and the earth ground, the transformer's CM EMI models are thus very important.

The famous two-capacitor transformer CM EMI model was first developed in [1,16] based on the conservation of the displacement current flowing through the distributed capacitance between windings or the energy conservation for the energy stored in the interwinding capacitances as in Fig. 9. It was disclosed by the model that the CM EMI noise flowing through the transformer windings is not due to the total CM capacitance between the primary and secondary windings but due to the capacitance ratio of the two capacitors in the model. Reducing the para-

sitic capacitance between windings therefore may not be able to efficiently reduce CM EMI noise.

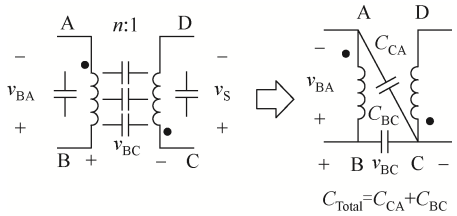


Fig. 9 Transformer's two-capacitor CM EMI model greatly helps the diagnosis and suppression of CM EMI due to switching transformers[16]

The CM EMI model for the ACF with the transformer's two-capacitor model is shown in Fig. 10[1,16], where the DC bus has a capacitor C_{DC} and the AC filter is a CM inductor L_{CM}. Based on the superposition theory, it was disclosed that only switching voltage V_{S_1} leads to CM EMI noise as shown in Fig. 10[1,16]. I_{S_2} and I_{S_3} can therefore be treated as open circuits.

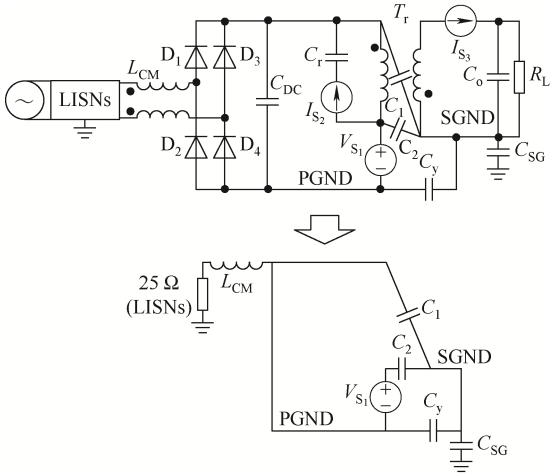


Fig. 10 Develop CM EMI model for flyback converters[1,16]

In high-power-density design, components are very close to each other, and the DC-bus filter is vulnerable to capacitive couplings from the voltage pulsating node as in Fig. 11(a) [11].

The CM noise bypasses the CM choke via the capacitive coupling C_{BD} between the pulsating node N_D and the quiet node N_B (including C_{DC}), and via C_{BC}. If the CM inductor is modeled as L_{CM}, EPC and EPR (equivalent parallel resistance), the CM EMI model is an unbalanced Wheatstone bridge as in Fig. 11(b), resulting in high CM EMI.

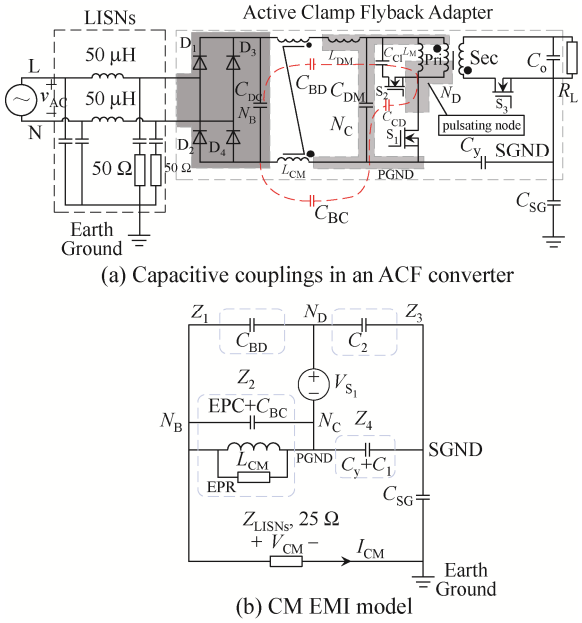


Fig. 11 Capacitive couplings in an ACF converter and CM EMI model[11]

For the CM EMI filter with grounded CM capacitors, the grounding impedance is important. For two-stage CM EMI filters, the common impedance of or the mutual inductance between two grounding paths are critical to CM filter's performance[25].

2.2.2 CM EMI Reduction

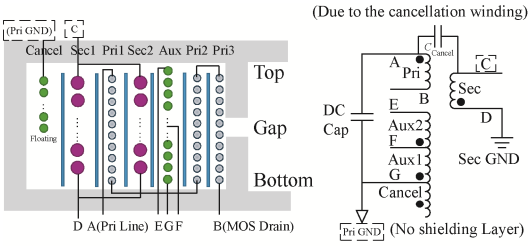
CM EMI can be reduced either from noise sources or from EMI propagation paths. The CM EMI can be reduced from noise sources using similar techniques to those of DM noise source reduction in Table 1. On the EMI propagation paths, CM EMI filter topologies are also designed based on impedance mismatch[41-42,53-54] like that in Table 1. At the component level, for transformers, CM EMI flowing from the primary winding to the secondary winding can be balanced by a CM current flowing from the secondary winding to the primary winding. For a CM EMI balanced transformer, C_2 in Fig. 10 is minimized. This can be achieved with a winding voltage distribution design, or with a cancellation winding[11,51,55-61], or with an external small cancellation capacitor[1,51]. Shielding

technique is also used between winding layers to either bypass CM EMI back to its source side or to eliminate the CM noise path on the magnetic core[1,62-65]. Either complete two-layer shielding or partial double shielding can be implemented with shielding foils based on the balancing conditions[13]. However, transformer shielding foils may have disadvantages: high eddy-current power loss in the shielding[66], high leakage inductance[1], and the increased manufacturing complexity and cost. For CM inductors, EPC cancellation can improve their HF performance[11,43,45]. These techniques are summarized in Table 2.

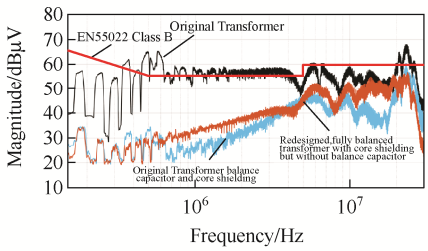
Tab. 2 CM conducted EMI noise reduction techniques

Techniques	Brief description
Transformer design for CM EMI reduction	Transformer CM noise balancing using cancellation windings[11,51,55-61] or external balancing capacitors[1,51] for wire-wound[1,11,55,67] and planar transformers[4,57-58,68-69]; CM voltage cancellation by inserting compensation voltage source into power lines using coupled windings[61,70]
	Shielding between primary and secondary windings to bypass CM noise back to its source, coaxial shielding to minimize interwinding voltage difference and to block capacitive couplings, core shielding to eliminate CM path on the core[1,62-65]
EMI filter design	EMI filter topology with impedance mismatch[41-42,53-54], EPC cancellation for CM inductors[11,43,45]
Parasitic coupling mitigation	Near electric-field (capacitive) coupling mitigation by shielding voltage pulsating nodes[11]

Fig. 12 illustrates an optimal winding structure with a cancellation winding to reduce CM EMI due to the transformer: the primary winding layer "Pri1" and two parallel secondary winding layers "Sec1" and "Sec2" are adjacent. Their winding direction should be designed to minimize the voltage difference between the primary and the secondary winding layers; also, a cancellation winding "Cancel" is designed to generate an equivalent cancellation capacitance C_{Cancel} to cancel the CM noise[1]. The primary auxiliary winding "Aux" is located between the primary layer "Pri2" and the secondary layer "Sec2" to reduce the CM EMI due to small voltage difference between the two layers.



(a) Optimal transformer winding structure with a cancellation winding

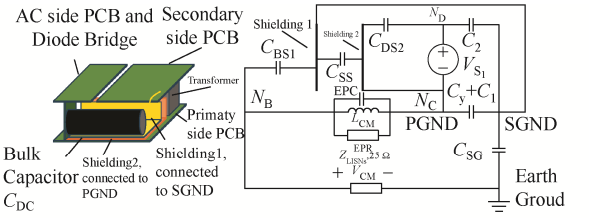


(b) Comparison of the measured CM noise

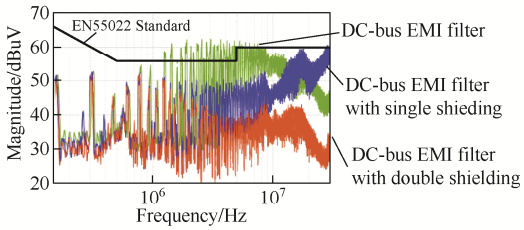
Fig. 12 Transformer winding optimization for CM EMI reduction[1]

The near electric-field (capacitive) couplings in Fig. 11 between bulk capacitor C_{DC} and transformer windings significantly degrade EMI filter performance due to the big size of C_{DC}. As shown in the flyback converter prototype in Fig. 13(a), a double shielding is used[11]: Shielding 1 connected to SGND is close to C_{DC}, and Shielding 2 connected to PGND is close to switching devices and the transformer with pulsating voltages. Shielding 1 is above Shielding 2. In Fig. 13(a), the transformer is modeled with the two-capacitor CM model C_1 and C_2, and the CM inductor L_{CM} is modeled with its EPR, EPC, and L_{CM}. The equivalent circuit in Fig. 13(a) illustrates that the double shielding technique can eliminate undesired capacitive couplings C_{BD} and C_{BC}, and create desired capacitive couplings C_{BS1} and C_{SS}, which perform like two CM filtering capacitors. As a result, the CM

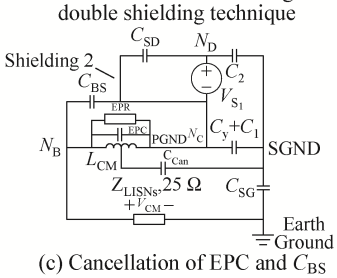
EMI is greatly reduced in Fig. 13(b). When there is a single shielding (Shielding 2) only, a parasitic capacitance C_{BS} between the shielding and node N_B is in parallel with the EPC of the CM inductor as in Fig. 13(c). CM EMI can be further reduced in Fig. 13(d) by cancelling these two capacitances with a cancellation capacitance C_{Can} connected between the center of the bifilar winding halves of the CM inductor and SGND as in Fig. 13(c)[11]. This is very valuable when the earth ground is unavailable for EPC cancellation techniques when power adapters use two-prong power plugs.



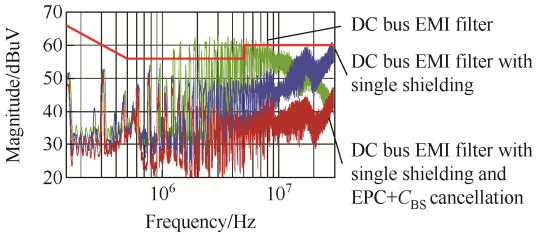
(a) Physical realization of double shielding, and its equivalent circuit



(b) Mcasured CM EMI for the converter in Fig. 11 with single and double shielding technique



(c) Cancellation of EPC and C_{BS}



(d) CM EMI reduction

Fig. 13 Comparison of single and double shielding techniques[11]

CM EMI can also be reduced by canceling CM voltages in Fig. 14[61] using a CM cancellation winding coupled with transformer windings to generate an inverse CM voltage.

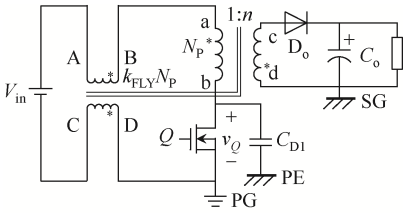


Fig. 14 CM voltage cancellation using cancellation windings coupled with transformer windings[61]

3 Modeling and Reduction of Radiated EMI

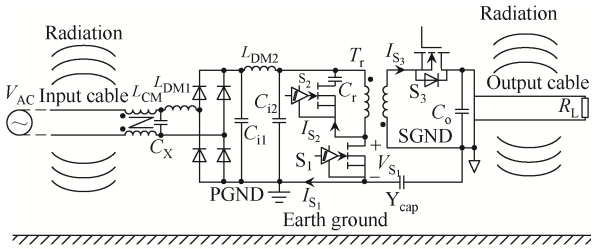
WBG devices, such as GaN high-electron-mobility transistor (HEMT), have been employed in flyback converters as in Fig. 15(a) to improve efficiency and power density. On the other hand, a high-switching-frequency, high-switching-speed, and high-power-density design leads to strong near-field couplings and high radiated EMI[8,17,71].

3.1 Modeling of Radiated EMI

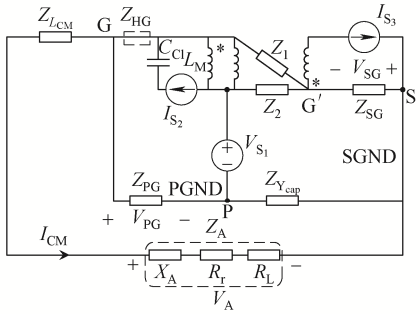
For the flyback converter with input and output power cables in Fig. 15(a), the power cables behave like an undesired antenna[18,72]. The antenna impedance Z_A includes a reactance X_A, representing the near-field energy between two cables, a resistance R_r, representing the radiated power, and a resistance R_L, representing the power loss. The antenna model is connected as a load of the flyback converter's EMI model. The radiated EMI can be predicted based on the power dissipated on R_r and the relationship between the radiated power, maximum electric field, antenna gain, and wave impedance[72].

The radiated EMI model is developed in Fig. 15(b) by replacing switching devices with current and vol-

tage sources, applying the transformer two-impedance (Z_1 and Z_2) CM EMI model[52], and connecting the cable antenna model Z_A across the input and output ports of the converter. Z_1 and Z_2 lead to a conversion from the DM voltage across the primary winding to the CM voltage between node S and G, resulting in an excitation voltage V_A added to Z_A, driving the cable to radiate EMI.



(a) A GaN IC-based ACF power adapter with power cables attached[17]

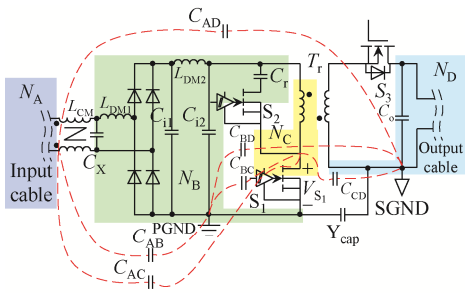


(b) Radiated EMI model with PCB ground impedances Z_{PG} and Z_{SG}[73]

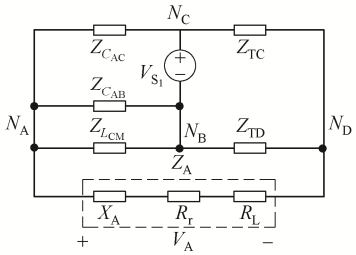
Fig. 15. GaN IC-based ACF power adapter with power cables attached and radiated EMI model with PCB ground impedances Z_{PG} and Z_{SG}

Z_{PG} and Z_{SG} are PCB ground impedances on primary and secondary sides, respectively. They cannot be ignored at high frequencies. Z_{PG} and Z_{SG} are critical PCB ground impedances that may also lead to excitation voltages added to the cable antenna, resulting in radiated EMI[73]. The HF switching currents I_{S_1} and I_{S_3} of switches S_1 and S_3 result in significant HF EMI voltage drops V_{PG} and V_{SG} on Z_{PG} and Z_{SG}. V_{PG} will be added between node G and S via Y capacitor Y_{cap}, whose impedance $Z_{Y_{cap}}$ is much smaller than that of the cable antenna. The conducted CM inductor L_{CM}'s impedance $Z_{L_{CM}}$ is smaller than the cable antenna impedance at high frequencies because of its winding capacitance[73], therefore, most of V_{PG} is added to the cable antenna for radiated EMI. In Fig. 15(b), V_{SG} does not lead to radiated EMI because Z_1 and Z_2 are much higher than $Z_{Y_{cap}}$. How Y_{cap} is connected to primary or secondary ground is important. If Y_{cap} is connected to G′ on secondary ground, V_{SG} will play a big role in radiated EMI. The voltage drop of switching current on Z_{HG} on the positive power path does not result in radiated EMI.

The near-field coupling in the flyback converter may also lead to radiated EMI[17]. In Fig. 16(a), the capacitive coupling C_{AC} between voltage pulsating node N_C and quiet node N_A, C_{AB} between nodes N_A and N_B and the CM inductor impedance $Z_{L_{CM}}$ form two branches of an equivalent Wheatstone bridge in Fig. 16(b). The other two branches Z_{TC} and Z_{TD} are the extracted two-impedance model for the network including both the transformer and Y_{cap}. The bridge is



(a) Identified voltage nodes and capacitive couplings in an ACF



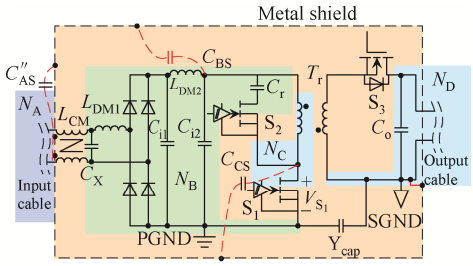
(b) Radiated EMI model including the capacitive couplings

Fig. 16 Radiated EMI model including critical capacitive couplings[17]

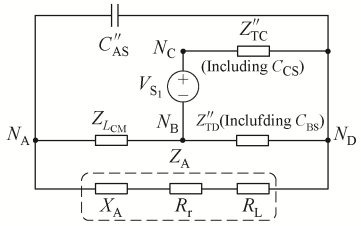
unbalanced, so the voltage between node N_A and N_D is not zero, resulting in radiated EMI.

3.2 Reduction of Radiated EMI

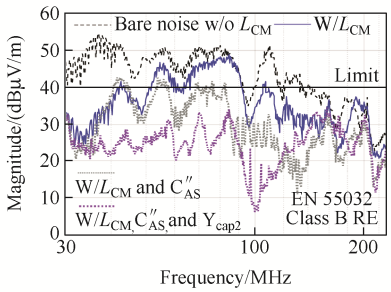
An improved transformer winding structure, such as coaxial shielding, can reduce the DM to CM conversion and radiated EMI[19]. Z_{PG} and Z_{SG} can be minimized with an optimal layout to reduce radiated EMI. Furthermore, the Y_{cap} can be connected between G and S in Fig. 15 to minimize the impacts of V_{PG} and V_{SG}, reducing radiated EMI. An improved shielding (metal shield) and grounding technique (grounded the shield to the SGND) in Fig. 17(a)[17] can block undesired capacitive couplings such as C_{AC} and C_{AB}, and create desired parasitic capacitance C''_{AS} between power cables and the shielding to reduce the radiation excitation, as in Fig. 17(a), (b), and (c).



(a) Improved shielding and grounding technique



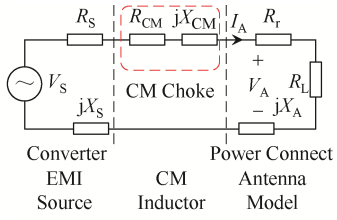
(b) Rradiated EMI model



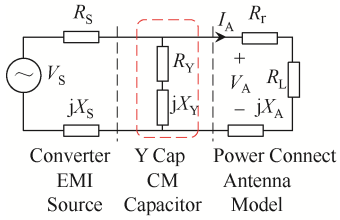
(c) Comparison of measured radiated EMI

Fig. 17 Mitigation of near electric-field (capacitive) **couplings**[17]

EMI filters are investigated to mitigate the radiated EMI in Fig. 18[74]. The impedance of filter inductors and capacitors should be designed to have desired magnitudes and phases at the desired frequencies to suppress noise and avoid resonances[43,53] due to their interactions with noise source impedances and the antenna impedance. As an example, the imaginary part of the loop impedance in Fig. 18(a) should not approach zero at the frequencies concerned using the CM inductor. The magnetic material of CM inductors including the inductance and high frequency loss resistance[75-78], the parasitics of the CM inductor[9,21,50], and the HF CM filter design and integration[79-80], should be considered according to the radiated EMI reduction requirement and the interactions with the noise source impedance and the antenna impedance[72,74].



(a) CM inductor



(b) CM capacitor

Fig. 18 Impedance design to suppress radiated EMI[74]

Inductor winding structures with minimized H-field emission and external magnetic field immunity have been investigated in[47-49] to reduce parasitic couplings and radiated EMI. Radiated EMI reduction techniques are listed in Table 3.

Tab. 3 Radiated EMI noise reduction techniques

Techniques	Brief description
Noise source reduction	Snubbers, soft-switching, gate driver circuits optimization[4,81]
Transformer winding structure optimization	Optimal winding design to reduce DM to CM conversion[19]
PCB layout optimization	Reduce critical ground impedance[73,82]; optimize component layout[83-84]
HF EMI filter design	HF CM capacitor and CM inductor impedance design and optimization[17,41,84]
Near-field coupling mitigation	Inductor winding design for near-field immunity[47-49], optimal shielding and grounding[17]

4 Conclusions and Future Research

This paper systematically summarizes the modeling and reduction techniques for conducted and radiated EMI in flyback converters.

To develop EMI models for flyback EMI, several steps should be followed: (1) develop the noise source model with the substitution theorem; (2) analyze the impacts of the noise sources to EMI with the superposition theorem, identify the major noise source and critical parameters; (3) determine EMI propagation paths and identify critical components; (4) explore and identify important inductive and capacitive near-field couplings.

To mitigate EMI, several steps should be followed: (1) mitigate the EMI due to the reverse recovery current of 50/60 Hz diode rectifier; (2) optimize components critical for EMI reduction, such as transformer winding structure or shielding design for CM noise mitigation; (3) design filter topology based on impedance mismatch rule, and optimize the filter component impedance; (4) reduce near-field couplings using winding structure, orientation, shielding or cancellation techniques.

The high switching speed of WBG devices will pose unique EMI challenges and bring research opportunities in WBG flyback converters as in Table 4.

Tab. 4 Challenges and research topics for WBG flyback converters

Challenges	Research topics
Conducted EMI modeling and reduction	Aim: Analyze noise source in WBG flyback converters Topics: Modeling of switching devices and DM-CM noise sources in flyback converters
	Aim: Reduce noise sources without reducing efficiency Topics: Optimization of switching devices, drivers, control and modulation, and component/system integration
	Aim: Reduce CM EMI with the transformer optimization Topics: Modeling and optimization of transformer windings at high frequencies, core material and winding structure optimization, CM EMI balancing and shielding
Radiated EMI modeling and reduction	Aim: Improve radiated EMI modeling Topics: Modeling of HF noise generation, conversion, and propagation in layout, transformers, filters, and antennas; HF modeling of components and near-field couplings
	Aim: Reduce radiated EMI Topics: Optimization of switching devices, driver circuits, transformer winding, core structures, PCB layouts, filters, and shielding
Near-field coupling effect mitigation	Aim: Investigate the effects of near-field couplings on conducted and radiated EMI Topics: Modeling of near-field couplings, and their effect on noise sources, conversion, and propagation paths
	Aim: To mitigate near-field coupling effects Topics: Component design with low near-field emissions and low susceptibility, PCB layout optimization, shielding and grounding optimization

References:

[1] Li Yiming, Zhang Huan, Wang Shuo, et al. Investigating switching transformers for common mode EMI reduction to remove common mode EMI filters and Y-capacitors in flyback converters [J]. IEEE Journal of Emerging and Selected Topics in Power Electronics, 2018, 6(4): 2287-2301.

[2] Li Jianting, van Horck F B M, Daniel B J, et al. A high-switching-frequency flyback converter in resonant mode [J]. IEEE Transactions on Power Electronics, 2017,

32(11): 8582-8592.

[3] Xue Lingxiao, Zhang J. Highly efficient secondaryresonant active clamp flyback converter [J]. IEEE Transactions on Industrial Electronics, 2018, 65(2): 1235- 1243.

[4] Huang Xiucheng, Feng Junjie, Du Weijing, et al. Design consideration of MHz active clamp flyback converter with GaN devices for low power adapter application [C]// 2016 IEEE Applied Power Electronics Conference and Exposition (APEC). Long Beach, CA, USA, 2016: 2334-2341.

[5] Zhang Junming, Huang Xiucheng, Wu Xinke, et al. A high efficiency flyback converter with new active clamp technique [J]. IEEE Transactions on Power Electronics, 2010, 25(7): 1775-1785.

[6] Huang Yingting, Li C H, Chen Y M. A modified asymmetrical half-bridge flyback converter for step-down AC-DC applications [J]. IEEE Transactions on Power Electronics, 2020, 35(5): 4613-4621.

[7] Li Mingxiao, Ouyang Ziwei, Andersen M A E. Analysis and optimal design of high-frequency and high-efficiency asymmetrical half-bridge flyback converters [J]. IEEE Transactions on Industrial Electronics, 2020, 67(10): 8312-8321.

[8] Zhang Boyi, Wang Shuo. A survey of EMI research in power electronics systems with wide-bandgap semiconductor devices [J]. IEEE Journal of Emerging and Selected Topics in Power Electronics, 2020, 8(1): 626-643.

[9] Wang Shuo, van Wyk J D, Lee F C. Effects of interactions between filter parasitics and power interconnects on EMI filter performance [J]. IEEE Transactions on Industrial Electronics, 2007, 54(6): 3344-3352.

[10] Wang Shuo, Lee F C, Odendaal W G. Characterization, evaluation, and design of noise separator for conducted EMI noise diagnosis [J]. IEEE Transactions on Power Electronics, 2005, 20(4): 974-982.

[11] Li Yiming, Wang Shuo, Sheng Honggang, et al. Investigate and reduce capacitive couplings in a flyback adapter with a DC-bus filter to reduce EMI [J]. IEEE Transactions on Power Electronics, 2020, 35(7): 6963-6973.

[12] Li Yiming, Yang Le, Wang Shuo, et al. Investigation of a DC bus differential mode EMI filter for AC/DC power adapters [C]// 2018 IEEE Applied Power Electronics Conference and Exposition (APEC). San Antonio, TX, USA, 2018: 603-610.

[13] Yang Yuchen, Huang Daocheng, Lee F C, et al. Transformer shielding technique for common mode noise reduction in isolated converters [C]// 2013 IEEE Energy Conversion Congress and Exposition. Denver, CO, USA, 2013: 4149-4153.

[14] Mainali K, Oruganti R. Conducted EMI mitigation techniques for switch-mode power converters: A survey [J]. IEEE Transactions on Power Electronics, 2010, 25(9): 2344-2356.

[15] Ma Zhedong, Li Yiming, Wang Shuo, et al. Investigation and reduction of EMI noise due to the reverse recovery currents of 50/60 Hz diode rectifiers [J]. IEEE Journal of Emerging and Selected Topics in Industrial Electronics, 2022, 3(3): 594-603.

[16] Zhang Huan, Wang Shuo, Li Yiming, et al. Two-capacitor transformer winding capacitance models for common-mode EMI noise analysis in isolated DC-DC converters [J]. IEEE Transactions on Power Electronics, 2017, 32(11): 8458-8469.

[17] Yao Juntao, Li Yiming, Wang Shuo, et al. Modeling and reduction of radiated EMI in a GaN IC-based active clamp flyback adapter [J]. IEEE Transactions on Power Electronics, 2021, 36(5): 5440-5449.

[18] Yao Juntao, Wang Shuo, Zhao Hui. Measurement techniques of common mode currents, voltages, and impedances in a flyback converter for radiated EMI diagnosis [J]. IEEE Transactions on Electromagnetic Compatibility, 2019, 61(6): 1997-2005.

[19] Yao Juntao, Li Yiming, Zhao Hui, et al. Modeling and reduction of radiated common mode current in flyback converters [C]// 2018 IEEE Energy Conversion Congress and Exposition (ECCE). Portland, OR, USA, 2018: 6613-6620.

[20] Ma Zhedong, Wang Shuo, Huang Qinghui, et al. A review of radiated EMI research in power electronics systems [J]. IEEE Journal of Emerging and Selected Topics in Power Electronics, 2024, 12(1): 675-694.

[21] Wang Shuo, Lee F C, Chen D Y, et al. Effects of parasitic

parameters on EMI filter performance [J]. IEEE Transactions on Power Electronics, 2004, 19(3): 869-877.

[22] Wang Shuo, Lee F C, Odendaal W G. Characterization and parasitic extraction of EMI filters using scattering parameters [J]. IEEE Transactions on Power Electronics, 2005, 20(2): 502-510.

[23] Wang Shuo, Lee F C, van Wyk J D. Design of inductor winding capacitance cancellation for EMI suppression [C]// 2006 37th IEEE Power Electronics Specialists Conference. Jeju, Korea, 2006: 1-7.

[24] Lai Rixin, Maillet Y, Wang F, et al. An integrated EMI choke for differential-mode and common-mode noise suppression [J]. IEEE Transactions on Power Electronics, 2010, 25(3): 539-544.

[25] Wang Shuo, Maillet Y Y, Wang Fei, et al. Parasitic effects of grounding paths on common-mode EMI filter's performance in power electronics systems [J]. IEEE Transactions on Industrial Electronics, 2010, 57(9): 3050-3059.

[26] Wang Shuo, Lee F C, van Wyk J D, et al. A study of integration of parasitic cancellation techniques for EMI filter design with discrete components [J]. IEEE Transactions on Power Electronics, 2008, 23(6): 3094-3102.

[27] Li Yiming, Wang Shuo. Modeling and increasing the high-frequency impedance of single-layer Mn-Zn ferrite toroidal inductors with electromagnetic analysis [J]. IEEE Transactions on Power Electronics, 2021, 36(6): 6943-6953.

[28] García-Caraveo A, Soto Á, González R, et al. Brief review on snubber circuits [C]// 2010 20th International Conference on Electronics Communications and Computers (CONIELECOMP). Cholula, Puebla, Mexico, 2010: 271-275.

[29] Meng Peipei, Wu Xinke, Yang Jianyou, et al. Analysis and design considerations for EMI and losses of RCD snubber in flyback converter [C]// 2010 Twenty-Fifth Annual IEEE Applied Power Electronics Conference and Exposition (APEC). Palm Springs, CA, USA, 2010: 642-647.

[30] Fiori F. On the use of magnetically coupled resonant snubbers to mitigate the electromagnetic emission of power switching circuits [J]. IEEE Transactions on Electromagnetic Compatibility, 2022, 64(1): 259-262.

[31] Mohammadian N, Yazdani M R. Half-bridge flyback converter with lossless passive snubber and interleaved technique [J]. IET Power Electronics, 2018, 11(2): 239-245.

[32] Jung S, Cho G H. Transformer coupled recycle snubber for high-efficiency offline isolated LED driver with on-chip primary-side power regulation [J]. IEEE Transactions on Industrial Electronics, 2014, 61(12): 6710-6719.

[33] Yau Y T, Hung T L. Lossless snubber for GaN-based flyback converter with common mode noise consideration [J]. IEEE Access, 2022, 10: 56652-56667.

[34] Yau Y T, Hung T L. A flyback converter with novel active dissipative snubber [J]. IEEE Access, 2022, 10: 108145-108158.

[35] Bodur H, Akboy E, Yeşilyurt H. A new and modular active snubber cell for inverters [J]. IEEE Transactions on Industrial Electronics, 2020, 67(1): 288-296.

[36] Yazdani M R, Farzanehfard H, Faiz J. EMI analysis and evaluation of an improved ZCT flyback converter [J]. IEEE Transactions on Power Electronics, 2011, 26(8): 2326-2334.

[37] Yazdani M R, Farzanehfard H. Conducted electromagnetic interference analysis and mitigation using zero-current transition soft switching and spread spectrum techniques [J]. IET Power Electronics, 2012, 5(7): 1034-1041.

[38] Mohammadi M, Adib E, Yazdani M R. Family of soft-switching single-switch PWM converters with lossless passive snubber [J]. IEEE Transactions on Industrial Electronics, 2014, 62(6): 3473-3481.

[39] Jung J H. Feed-forward compensator of operating frequency for APWM HB flyback converter [J]. IEEE Transactions on Power Electronics, 2012, 27(1): 211-223.

[40] Park H P, Jeong S, Kim M, et al. Spread spectrum technique for decreasing EM noise in high-frequency APWM HB resonant converter with reduced EMI filter size [J]. IEEE Transactions on Power Electronics, 2019, 34(11): 10845-10855.

[41] Luo Fang, Dong Dong, Boroyevich D, et al. Improving

high-frequency performance of an input common mode EMI filter using an impedance-mismatching filter [J]. IEEE Transactions on Power Electronics, 2014, 29(10): 5111-5115.

[42] Luo Fang, Baisden A C, Boroyevich D, et al. Design of a hybrid busbar filter combining a transmission-line busbar filter and a one-turn inductor for DC-fed three-phase motor drive systems [J]. IEEE Transactions on Power Electronics, 2013, 28(12): 5588-5602.

[43] Wang Shuo, Chen Rengang, van Wyk J D, et al. Developing parasitic cancellation technologies to improve EMI filter performance for switching mode power supplies [J]. IEEE Transactions on Electromagnetic Compatibility, 2005, 47(4): 921-929.

[44] Wang Shuo, Lee F C. Analysis and applications of parasitic capacitance cancellation techniques for EMI suppression [J]. IEEE Transactions on Industrial Electronics, 2009, 57(9): 3109-3117.

[45] Li Yiming, Wang Shuo, Shen Honggang, et al. Inductor winding capacitance cancellation for flyback converters without grounding paths [C]// 2020 IEEE International Symposium on Electromagnetic Compatibility & Signal/Power Integrity (EMCSI). Reno, NV, USA, 2020: 640-645.

[46] Wang Shuo, Lee F C, Odendaal W G. Cancellation of capacitor parasitic parameters for noise reduction application [J]. IEEE Transactions on Power Electronics, 2006, 21(4): 1125-1132.

[47] Lai Yanwen, Wang Shuo, Zhang Boyi. Investigation of magnetic field immunity and near magnetic field reduction for the inductors in high power density design [J]. IEEE Transactions on Power Electronics, 2019, 34(6): 5340-5351.

[48] Zhang Boyi, Wang Shuo. Analysis and reduction of the near magnetic field emission from toroidal inductors [J]. IEEE Transactions on Power Electronics, 2020, 35(6): 6251-6268.

[49] Chu Yongbin, Wang Shuo, Zhang Ning, et al. A common mode inductor with external magnetic field immunity, low-magnetic field emission, and high-differential mode inductance [J]. IEEE Transactions on Power Electronics, 2015, 30(12): 6684-6694.

[50] Wang S, Lee F C, Odendaal W G, et al. Improvement of EMI filter performance with parasitic coupling cancellation [C]// 2005 IEEE 36th Power Electronics Specialists Conference. Dresden, Germany, 2005: 1780-1786.

[51] Huang Qinghui, Yang Yirui, Ma Zhedong, et al. Transformer structure of bifilar primary winding with advanced common mode noise attenuation performance for isolated DC-DC converters [C]// 2023 IEEE Applied Power Electronics Conference and Exposition (APEC). Orlando, FL, USA, 2023: 441-448.

[52] Huang Qinghui, Li Yiming, Ma Zhedong, et al. RLC balance technique of transformer to reduce CM EMI for isolated DC-DC converters [C]// 2023 IEEE Energy Conversion Congress and Exposition (ECCE). Nashville, TN, USA, 2023: 2945-2952.

[53] Huang Fan, Hui Qi, Ren Xiaoyong, et al. Analytical modeling and worst case analysis of common-mode EMI spectrum in quasi-resonant flyback converters [J]. IEEE Journal of Emerging and Selected Topics in Power Electronics, 2025, 13(2): 2036-2045.

[54] Hubert F, Dorsch P, Kuebrich D, et al. Piezoelectric EMI filter for switched-mode power supplies [J]. IEEE Transactions on Power Electronics, 2021, 36(6): 6624-6643.

[55] Chu Yongbin, Wang Shuo. A generalized common-mode current cancelation approach for power converters [J]. IEEE Transactions on Industrial Electronics, 2015, 62(7): 4130-4140.

[56] Chan Y P, Pong B M H, Poon N K, et al. Common-mode noise cancellation in switching-mode power supplies using an equipotential transformer modeling technique [J]. IEEE Transactions on Electromagnetic Compatibility, 2012, 54(3): 594-602.

[57] Chan Y P, Pong B M H, Poon N K, et al. Common-mode noise cancellation by an antiphase winding in multilayer isolated planar transformer [J]. IEEE Transactions on Electromagnetic Compatibility, 2014, 56(1): 67-73.

[58] Ali Saket M, Ordonez M, Shafiei N. Planar transformers with near-zero common-mode noise for flyback and forward converters [J]. IEEE Transactions on Power Electronics, 2018, 33(2): 1554-1571.

[59] Chen Henglin, Zheng Zhichao, Xiao Ji. Determining the number of transformer shielding winding turns for suppressing common-mode noise in flyback converters [J]. IEEE Transactions on Electromagnetic Compatibility, 2018, 60(5): 1606-1609.

[60] Bai Yongjiang, Yang Xu, Zhang Dan, et al. Conducted EMI mitigation schemes in isolated switching-mode power supply without the need of a Y-capacitor [J]. IEEE Transactions on Power Electronics, 2016, 32(4): 2687-2703.

[61] Xie Lihong, Ruan Xinbo, Zhu Haonan, et al. Common-mode voltage cancellation for reducing the common-mode noise in DC-DC converters [J]. IEEE Transactions on Industrial Electronics, 2021, 68(5): 3887-3897.

[62] Xie Lihong, Ruan Xinbo, Ji Qing, et al. Shielding-cancelation technique for suppressing common-mode EMI in isolated power converters [J]. IEEE Transactions on Industrial Electronics, 2015, 62(5): 2814-2822.

[63] Fei Chao, Yang Yuchen, Li Qiang, et al. Shielding technique for planar matrix transformers to suppress common-mode EMI noise and improve efficiency [J]. IEEE Transactions on Industrial Electronics, 2018, 65(2): 1263-1272.

[64] Chen Henglin, Xiao Ji. Determination of transformer shielding foil structure for suppressing common-mode noise in flyback converters [J]. IEEE Transactions on Magnetics, 2016, 52(12): 8401809.

[65] Chen Henglin, Liu Guanchen. Determination of the width of shielding foil in sandwiched winding transformer for minimizing common mode EMI of flyback converters [J]. IEEE Transactions on Electromagnetic Compatibility, 2020, 62(2): 639-642.

[66] Shen Zhan, Kaymak M, Wang Huai, et al. The faraday shields loss of transformers [J]. IEEE Transactions on Power Electronics, 2020, 35(11): 12194-12206.

[67] Zhao Dingkun, Pei Xuejun, Yu Yi, et al. CM noise modeling and reduction for multi-output dual-switch flyback auxiliary power supplies [J]. IEEE Transactions on Industry Applications, 2024, 61(1): 429-438.

[68] Ali Saket M, Ordonez M, Craciun M, et al. Improving planar transformers for LLC resonant converters: Paired layers interleaving [J]. IEEE Transactions on Power Electronics, 2019, 34(12): 11813-11832.

[69] Kim K W, Jeong Y, Kim J S, et al. Low common-mode noise full-bridge LLC resonant converter with balanced resonant tank [J]. IEEE Transactions on Power Electronics, 2021, 36(4): 4105-4115.

[70] Fu Dianbo, Wang Shuo, Kong Pengju, et al. Novel techniques to suppress the common-mode EMI noise caused by transformer parasitic capacitances in DC-DC converters [J]. IEEE Transactions on Industrial Electronics, 2013, 60(11): 4968-4977.

[71] Yao Juntao, Lai Yanwen, Ma Zhedong, et al. Investigation of noise spectrum and radiated EMI in high switching frequency flyback converters [C]// 2021 IEEE Applied Power Electronics Conference and Exposition (APEC). Phoenix, AZ, USA, 2021: 2265-2270.

[72] Zhang Yingjie, Wang Shuo, Chu Yongbin. Investigation of radiated electromagnetic interference for an isolated high-frequency DC-DC power converter with power cables [J]. IEEE Transactions on Power Electronics, 2019, 34(10): 9632-9643.

[73] Ma Zhedong, Wang Shuo, Sheng Honggang, et al. Modeling, analysis and mitigation of radiated EMI due to PCB ground impedance in a 65 W high-density active-clamp flyback converter [J]. IEEE Transactions on Industrial Electronics, 2023, 70(12): 12267-12277.

[74] Zhang Yingjie, Wang Shuo. Characterization and design of filter inductors and capacitors to suppress the radiated EMI in a power converter [C]// 2022 International Power Electronics Conference (IPEC-Himeji 2022- ECCE Asia). Himeji, Japan, 2022: 1082-1089.

[75] Kovacic M, Hanic Z, Stipetic S, et al. Analytical wideband model of a common-mode choke [J]. IEEE Transactions on Power Electronics, 2012, 27(7): 3173-3185.

[76] Um D Y, Park G S. Resistance variations in high-frequency inductors considering induced fields among conductors [J]. IEEE Transactions on Magnetics, 2021, 57(2): 8400105.

[77] Sonehara M, Sato T. Relation between high-frequency properties and direction of anisotropy magnetic field in

magnetic thin film for RF inductor applications [J]. IEEE Transactions on Magnetics, 2012, 48(11): 4515-4517.

[78] Roc'h A, Leferink F. Optimization of the in situ performance of common mode chokes for power drive systems using designable parameters [J]. IEEE Transactions on Electromagnetic Compatibility, 2018, 60(2): 529-535.

[79] Jia Niu, Tian Xingyue, Xue Lingxiao, et al. Integrated common-mode filter for GaN power module with improved high-frequency EMI performance [J]. IEEE Transactions on Power Electronics, 2023, 38(6): 6897-6901.

[80] Menzi D, Bortis D, Kolar J W. EMI filter design for a three-phase Buck-Boost Y-inverter VSD with unshielded motor cables considering IEC 61800-3 conducted and radiated emission limits [J]. IEEE Transactions on Power Electronics, 2021, 36(11): 12919-12937.

[81] Middelstaedt L, Wang Jianjing, Stark B H, et al. Direct approach of simultaneously eliminating EMI-critical oscillations and decreasing switching losses for wide bandgap power semiconductors [J]. IEEE Transactions on Power Electronics, 2019, 34(11): 10376-10380.

[82] Yao Juntao, Wang Shuo, Luo Zheng. Modeling, analysis, and reduction of radiated EMI due to the voltage across input and output cables in an automotive non-isolated power converter [J]. IEEE Transactions on Power Electronics, 2022, 37(5): 5455-5465.

[83] Ma Zhedong, Lai Yanwen, Huang Qinghui, et al. Investigation and mitigation of radiated EMI due to near-field coupling in a high-density active-clamp flyback power adapter [C]// 2023 IEEE Energy Conversion Congress and Exposition (ECCE). Nashville, TN, USA, 2023: 2953-2958.

[84] Yao Juntao, Li Yiming, Zhao Hui, et al. Design of CM inductor based on core loss for radiated EMI reduction in power converters [C]// 2019 IEEE Applied Power Electronics Conference and Exposition (APEC). Anaheim, CA, USA, 2019: 2673-2680.



姚俊涛

作者简介：

姚俊涛(1989—)，男，博士，工程师。研究方向：电力电子，电磁干扰与电磁兼容。E-mail：juntao.yao@outlook.com。

王硕(1972—)，男，通信作者，博士，教授。研究方向：电力电子，电磁干扰/兼容，电磁安全，磁元件，功率器件封装。E-mail：shuowang@ieee.org。

(责任编辑：郭凯凯)